Acta Cryst E CRYSTALLOGRAPHIC COMMUNICATIONS

ISSN 2056-9890

Crystal structure and Hirshfeld surface analysis of 2,4-diamino-6-[(1*Z*,3*E*)-1-cyano-2,4-diphenylpenta-1,3-dien-1-yl]pyridine-3,5-dicarbonitrile monohydrate

Ibrahim G. Mamedov,[a] Victor N. Khrustalev,[b,c] Mehmet Akkurt,[d] Fuad Sh. Kerimli,[a] Ajaya Bhattarai,[e]* Ali N. Khalilov[f,a] and Farid N. Naghiyev[a]

[a]Department of Chemistry, Baku State University, Z. Khalilov str. 23, Az, 1148, Baku, Azerbaijan, [b]Peoples' Friendship University of Russia (RUDN University), Miklukho-Maklay St. 6, Moscow, 117198, Russian Federation, [c]N. D. Zelinsky Institute of Organic Chemistry RAS, Leninsky Prosp. 47, Moscow, 119991, Russian Federation, [d]Department of Physics, Faculty of Sciences, Erciyes University, 38039 Kayseri, Türkiye, [e]Department of Chemistry, M.M.A.M.C (Tribhuvan University) Biratnagar, Nepal, and [f]"Composite Materials" Scientific Research Center, Azerbaijan State Economic University (UNEC), H. Aliyev str. 135, Az 1063, Baku, Azerbaijan. *Correspondence e-mail: ajaya.bhattarai@mmamc.tu.edu.np

Received 26 February 2024
Accepted 6 April 2024

Edited by Y. Ozawa, University of Hyogo, Japan

Keywords: crystal structure; hydrogen bonds; pyridine ring; C—H···π interactions; Hirshfeld surface analysis.

CCDC reference: 2347583

Supporting information: this article has supporting information at journals.iucr.org/e

The asymmetric unit of the title compound, $C_{25}H_{18}N_6{\cdot}H_2O$, comproses two molecules (**I** and **II**), together with a water molecule. The terminal phenyl groups attached to the methyl groups of the molecules **I** and **II** do not overlap completely, but are approximately perpendicular. In the crystal, the molecules are connected by N—H···N, C—H···N, O—H···N and N—H···O hydrogen bonds with each other directly and through water molecules, forming layers parallel to the (001) plane. C—H···π interactions between these layers ensure the cohesion of the crystal structure. A Hirshfeld surface analysis indicates that H···H (39.1% for molecule **I**; 40.0% for molecule **II**), C···H/H···C (26.6% for molecule **I** and 25.8% for molecule **II**) and N···H/H···N (24.3% for molecules **I** and **II**) interactions are the most important contributors to the crystal packing.

1. Chemical context

Functionalized pyridines are six-membered heterocyclic systems containing one or several functional groups in their core. These derivatives are used for a large range of applications and as as drugs, ligands, catalysts, materials *etc* (Maharramov *et al.*, 2021; Sobhi & Faisal, 2023). Functionalized pyridines with various biological activities, such as anticancer, antioxidant, vasodilatory, cytotoxic, anti-inflammatory, herbicidal, insecticidal, antihypertensive, antibacterial, anticonvulsant, cardiotonic properties, as well as multiple synthetic pathways of these systems, have been reported (Atalay *et al.*, 2022; Donmez & Turkyılmaz, 2022; Abd El-Lateef *et al.*, 2023). Given the wide application of these compounds, the efficient and regioselective functionalization of pyridines has attracted much attention. Thus, in the framework of our studies in heterocyclic chemistry (Naghiyev *et al.*, 2020, 2021, 2022), herein we report the crystal structure and Hirshfeld surface analysis of the title compound, 2,4-diamino-6-[(1*Z*,3*E*)-1-cyano-2,4-diphenylpenta-1,3-dien-1-yl]-pyridine-3,5-dicarbonitrile. The plausible reaction mechanism of the formation of the title compound is illustrated in Fig. 1.

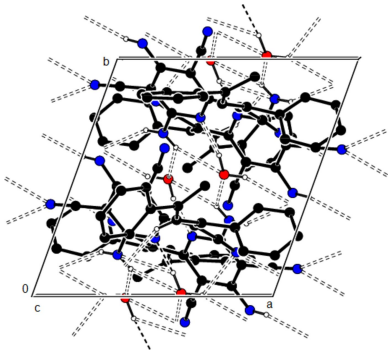

2. Structural commentary

Fig. 2 shows two molecules (**I** without suffix and **II** with suffix *A*), which together with a water molecule form the asymmetric unit. An overlay fit of inverted molecule **II** on molecule **I** is shown in Fig. 3, the weighted r.m.s. fit of the 31 non-H atoms being 0.510 Å and showing the major differences to be in the terminal phenyl groups (C20–C25 and C20*A*–C25*A*) attached to the methyl groups of the molecules **I** and **II**.

In **I**, the phenyl rings (C14–C19 and C20–C25) form a dihedral angle of 45.39 (11)° with each other, while they subtend angles of 80.43 (10) and 57.35 (10)°, respectively, with the pyridine ring (N1/C2–C6). In **II**, the phenyl rings (C14*A*–C19*A* and C20*A*–C25*A*) form a dihedral angle of 87.88 (11)° with each other, while they subtend angles of 76.94 (11) and 62.05 (10)°, respectively, with the pyridine ring (N1*A*/C2*A*–C6*A*). In **I**, the C6—C9—C10—C14, C6—C9—C10—C11, C9—C10—C11—C12 and C10—C11—C12—C20 torsion angles are 177.30 (18), −11.2 (3), 153.8 (2) and 174.73 (19)°, respectively. In **II**, the corresponding C6*A*—C9*A*—C10*A*—C14*A*, C6*A*—C9*A*—C10*A*—C11*A*, C9*A*—C10*A*—C11*A*—C12*A* and C10*A*—C11*A*—C12*A*—C20*A* torsion angles have approximately the same values, *viz*. 172.10 (19), −15.5 (3), 153.0 (2) and 173.0 (2)°, respectively. Bond lengths and angles in the molecules of the title compound are comparable with those of closely related structures detailed in the *Database survey* (section 4).

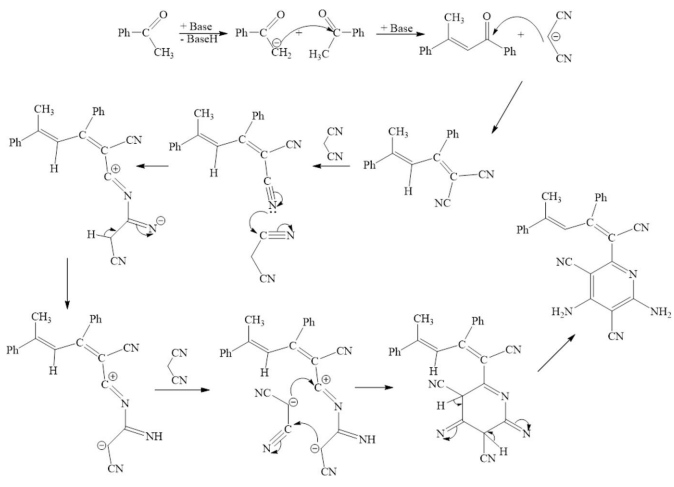

Figure 1
The plausible formation mechanism of the title compound.

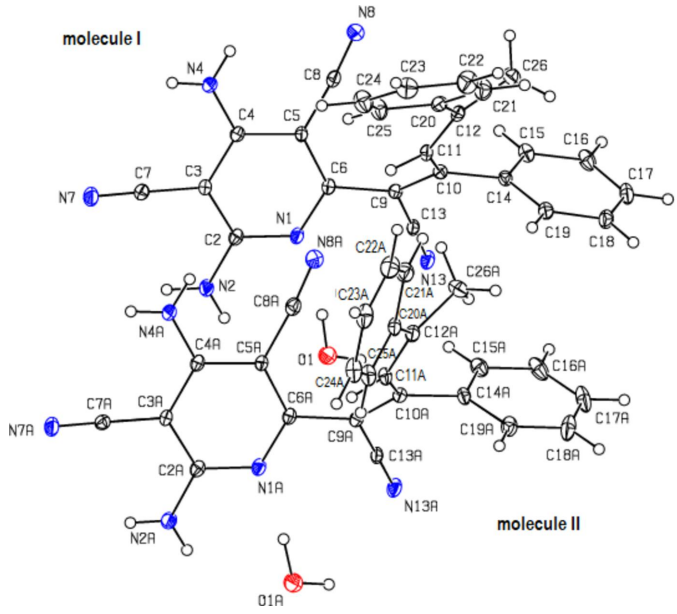

Figure 2
The molecular structure of the title compound, showing the atom labelling and displacement ellipsoids drawn at the 30% probability level.

3. Supramolecular features and Hirshfeld surface analysis

In the crystal, the molecules are connected by N—H···N and C—H···N and O—H···N and N—H···O hydrogen bonds with each other directly and through water molecules, forming

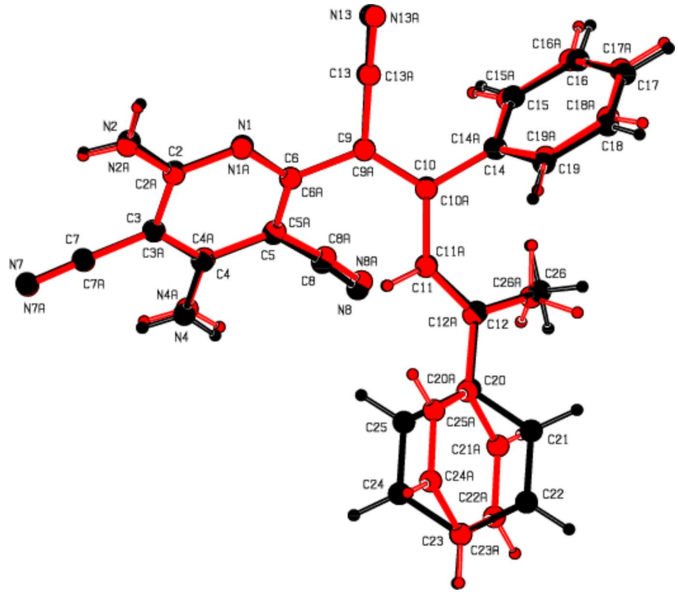

Figure 3
A least-squares overlay of the two independent molecules **I** and **II** [inverted molecule **II** (red) on molecule **I** (black)].

Table 1
Hydrogen-bond geometry (Å, °).

*Cg*5 and *Cg*6 are the centroids of the C14*A*–C19*A* and C20*A*–C25*A* phenyl rings of molecule **II**, respectively.

D—H···*A*	*D*—H	H···*A*	*D*···*A*	*D*—H···*A*
O1—H1*A*···N1	0.93 (2)	1.93 (2)	2.853 (2)	169 (3)
O1—H1*B*···N7*A*^{i}	0.89 (2)	2.33 (2)	3.163 (3)	156 (3)
O1*A*—H1*C*···N1*A*	1.04 (2)	1.78 (2)	2.811 (3)	174 (2)
O1*A*—H1*D*···N7^{ii}	0.91 (2)	2.38 (2)	3.206 (3)	152 (2)
O1*A*—H1*D*···N13*A*	0.91 (2)	2.59 (2)	3.153 (3)	121 (2)
N2—H2*A*···O1	0.86 (3)	2.44 (3)	3.140 (3)	139 (2)
N2—H2*A*···O1^{iii}	0.86 (3)	2.29 (3)	2.892 (3)	127 (2)
N2—H2*B*···N7*A*^{iv}	0.87 (3)	2.41 (3)	3.209 (3)	151.7 (18)
N2*A*—H2*C*···O1*A*	0.87 (3)	2.48 (3)	3.174 (3)	137 (2)
N2*A*—H2*C*···O1*A*^{v}	0.87 (3)	2.25 (3)	2.859 (3)	127 (3)
N2*A*—H2*D*···N7^{iv}	0.85 (3)	2.42 (3)	3.205 (3)	154 (3)
N4—H4*A*···N13*A*^{vi}	0.82 (3)	2.21 (3)	2.984 (3)	158 (3)
N4*A*—H4*C*···N13^{vii}	0.84 (3)	2.16 (3)	2.930 (3)	152 (2)
C11—H11···N8*A*	0.95	2.59	3.453 (3)	151
C11*A*—H11*A*···N8^{viii}	0.95	2.49	3.369 (3)	154
C21—H21···*Cg*6^{ix}	0.95	2.91	3.653 (2)	136
C26*A*—H26*F*···*Cg*5	0.98	2.97	3.781 (2)	141

Symmetry codes: (i) $x-1, y, z$; (ii) $x-1, y+1, z$; (iii) $-x+1, -y+1, -z+1$; (iv) $-x+2, -y+1, -z+1$; (v) $-x+1, -y+2, -z+1$; (vi) $x+1, y-1, z$; (vii) $x+1, y, z$; (viii) $x, y+1, z$; (ix) $-x+1, -y+1, -z$.

layers parallel to the (001) plane (Table 1; Figs. 4, 5 and 6). In addition, C—H···π interactions between these layers ensure the cohesion of the crystal structure (Table 1; Fig. 7).

Crystal Explorer 17.5 (Spackman *et al.*, 2021) was used to generate Hirshfeld surfaces for both independent molecules.

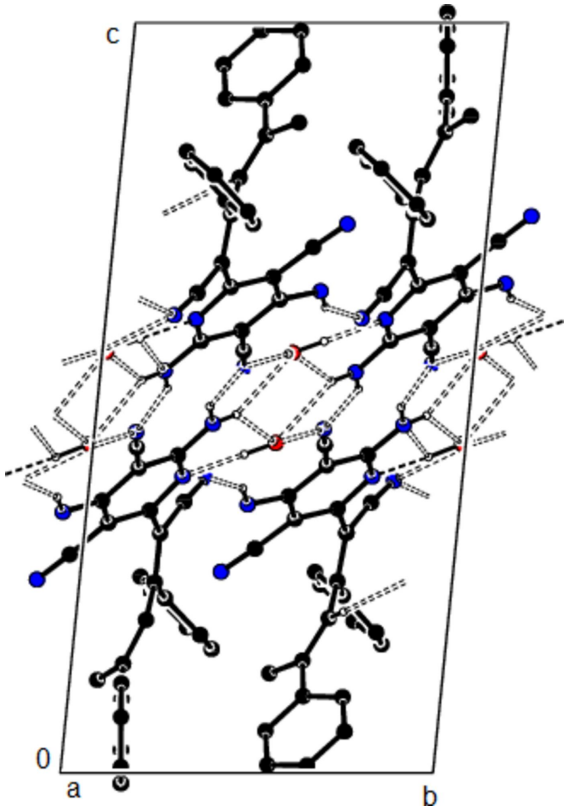

Figure 4
The packing of the title compound viewed along the *a* axis with O—H···N, N—H···O, N—H···N and C—H···N hydrogen bonds shown as dashed lines.

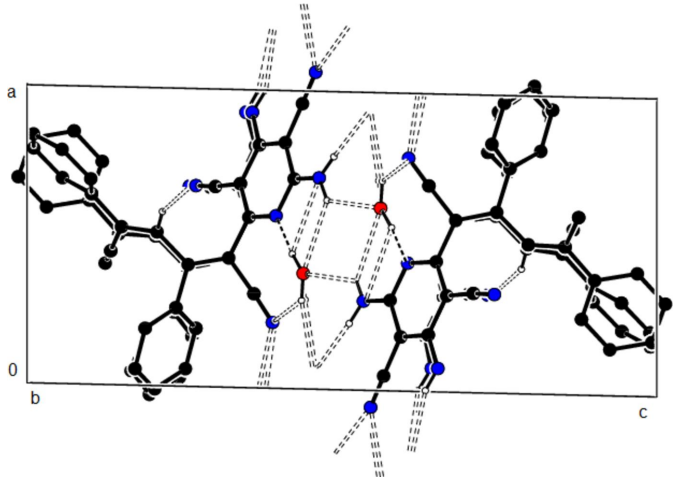

Figure 5
The packing of the title compound viewed along the *b* axis with O—H···N, N—H···O, N—H···N and C—H···N hydrogen bonds shown as dashed lines.

The d_{norm} mappings for molecules **I** and **II** were performed in the ranges −0.5788 to 1.4167 a.u. and −0.621 to 1.3731 a.u., respectively. The O—H···N, N—H···O, N—H···N and C—H···N interactions are indicated by red areas on the Hirshfeld surfaces (Fig. 8*a*,*b* for **I** and Fig. 8*c*,*d* for **II**). Although H···H interactions (39.1% for molecule **I** and 40.0% for molecule **II**) contribute the most to surface contacts, fingerprint plots (Fig. 9) show that C···H/H···C interactions (26.6% for molecule **I** and 25.8% for molecule **II**) and N···H/H···N interactions (24.3% for molecules **I** and **II**) are also significant (Tables 1 and 2). Other, less notable contacts are C···N/N···C (4.6% for molecule **I** and 4.4% for molecule **II**),

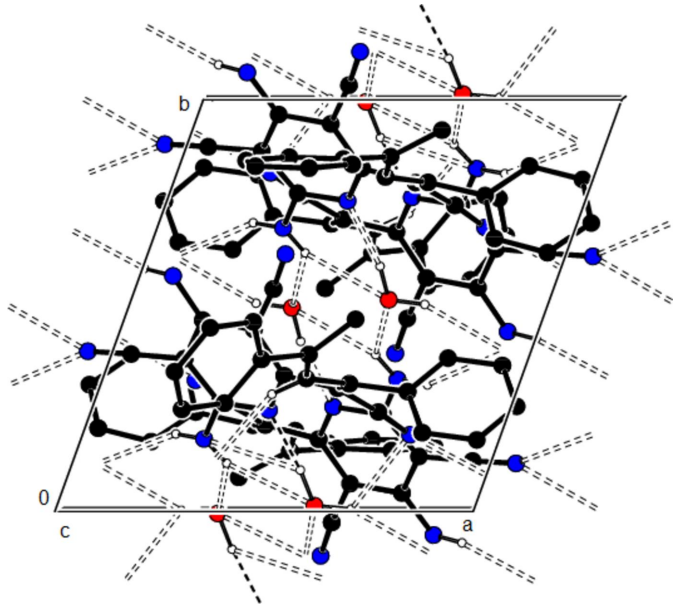

Figure 6
The packing of the title compound viewed along the *c* axis with O—H···N, N—H···O, N—H···N and C—H···N hydrogen bonds shown as dashed lines.

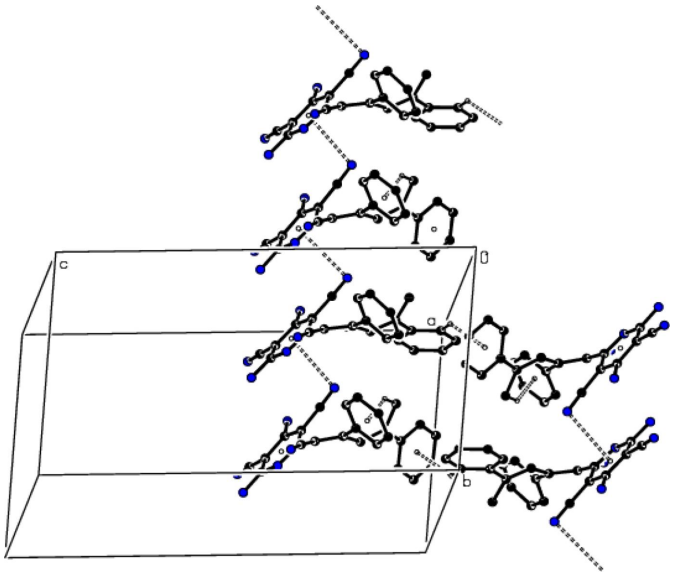

Figure 7
A view of the packing of the title compound along the *a* axis with C—H···π interactions shown as dashed lines.

N···N (1.9% contribution for molecule **I** and 2.0% for molecule **II**), O···H/H···O interactions (1.6% for molecule **I** and

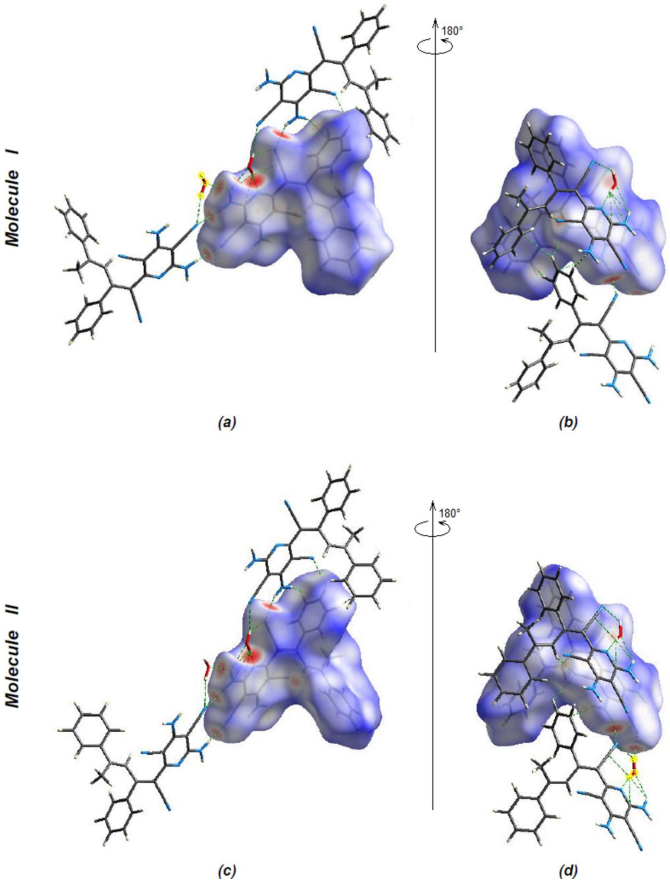

Figure 8
(*a*) Front and (*b*) back sides of the three-dimensional Hirshfeld surface of the title compound mapped over d_{norm} for **I**, (*c*) front and (*d*) back sides for **II**.

Table 2
Interatomic contacts of the title compound (Å).

N1···H1*A*	1.93	*x*, *y*, *z*
H19···H26*F*	2.48	*x*, *y*, *z*
H2*A*···O1	2.29	1 − *x*, 1 − *y*, 1 − *z*
H2*B*···N7*A*	2.41	2 − *x*, 1 − *y*, 1 − *z*
N13···H2*D*	2.67	1 − *x*, 1 − *y*, 1 − *z*
H4*A*···N13*A*	2.21	1 + *x*, −1 + *y*, *z*
N4···H16	2.90	1 + *x*, *y*, *z*
N7···H1*D*	2.38	1 + *x*, −1 + *y*, *z*
C7···N7	3.21	2 − *x*, −*y*, 1 − *z*
H26*B*···H25*A*	2.43	*x*, −1 + *y*, *z*
N13···H4*C*	2.16	−1 + *x*, *y*, *z*
C13···O1*A*	3.01	*x*, −1 + *y*, *z*
H22···H19*A*	2.37	1 − *x*, 1 − *y*, −*z*
N1*A*···H1*C*	1.78	*x*, *y*, *z*
H2*C*···O1*A*	2.25	1 − *x*, 2 − *y*, 1 − *z*
N4*A*···H16*A*	2.69	1 + *x*, *y*, *z*
N7*A*···H1*B*	2.33	1 + *x*, *y*, *z*
C7*A*···N7*A*	3.21	2 − *x*, 1 − *y*, 1 − *z*
C13*A*···O1	3.06	*x*, *y*, *z*

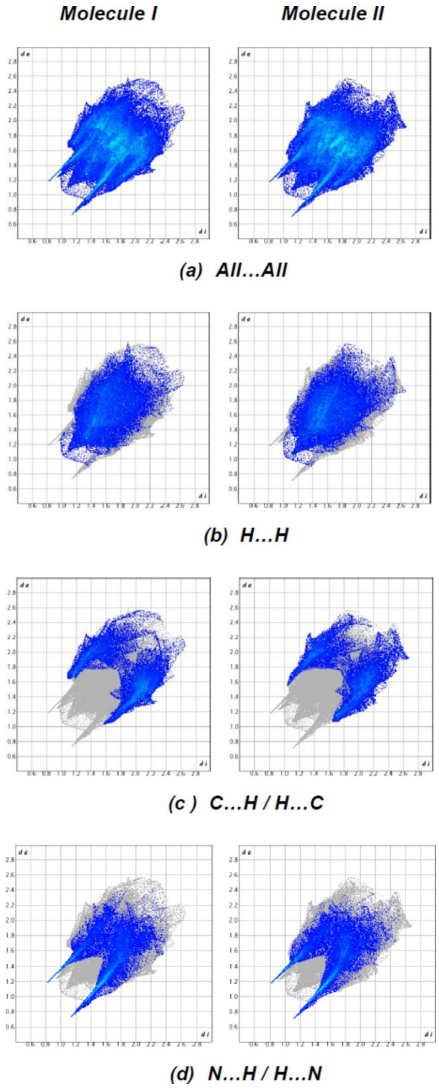

Figure 9
The two-dimensional fingerprint plots, showing (*a*) all interactions, and delineated into (*b*) H···H, (*c*) C···H/H···C and (*d*) N···H/H···N interactions. [d_e and d_i represent the distances from a point on the Hirshfeld surface to the nearest atoms outside (external) and inside (internal) the surface, respectively.]

1.7% for molecule **II**), O···C/C···O interactions (1.0% for molecules **I** and **II**), C···C (0.7% for molecule **I** and 0.8% for molecule **II**) and O···N/N···O interactions (0.1% for molecules **I** and **II**). A comparison of the supplied data shows that molecules **I** and **II** have extremely comparable environments.

4. Database survey

A search of the Cambridge Structural Database (CSD, version 5.43, update June 2022; Groom *et al.*, 2016) for the *buta-1,3-diene* unit gave ten similar structures, *viz.* CSD refcode SESRUE (Ibis & Deniz, 2006), JEYVAL (Ibis & Deniz, 2007*a*), SINDOJ (Ibis & Deniz, 2007*b*), WIHFAV (Ibis & Deniz, 2007*c*), CICMIL (Sathiyanarayanan *et al.*, 2007), GISDOC (Sathiyanarayanan *et al.*, 2008*a*), GIRQEE (Sathiyanarayanan *et al.*, 2008*b*), IGANUA (Bats *et al.*, 2008), KABKAB (Narayan *et al.*, 2010) and IDOTOM (Okuno & Iwahashi, 2013).

In SESRUE, the butadiene has a conformation closer to cisoid than to transoid, the C4—C3—C2—C1 torsion angle being −64.3 (3)°. In JEYVAL, the butadiene unit has assumed a configuration close to cisoid, but it is not completely planar. The C18—C19— C20—C21 torsion angle is −56.0 (11)°. In SINDOJ, the butadiene unit is not completely planar. The torsional angle of the butadiene unit (C1—C2—C3—C4) is −82.2 (5)°. In WIHFAV, the butadiene unit has assumed a configuration close to cisoid, but is not completely planar. The C4—C3—C2—C1 torsion angle is −97.2 (3)°. In CICMIL, cooperative C—H···π interactions form molecular dimers. The dimers associate in a one-dimensional chain along the *a*-axis direction. In GISDOC, the torsion angles describing the molecular conformation namely, C2—C1—O1—C7, C8—C7—O1—C1 and O1—C7—C8—C8^{i} [symmetry code: (i) $1-x, 1-y, -z$] are *trans*, *gauche* and *trans*, respectively. The structure is consolidated by a short intramolecular C—H···O contact. The molecules are held together by C—H···π interactions, forming a sheet structure parallel to the (201) plane. The structure of GIRQEE is consolidated by a short intermolecular C—H···O contact. Cooperative C—H···π interactions generate an infinite one-dimensional chains of molecules along the *a*-axis direction. In IGANUA, the asymmetric unit contains two half-molecules. Both complete molecules are generated by crystallographic inversion centres located at the mid-points of the central C—C single bonds; the butadiene groups are planar, with a *trans* conformation about the central C—C bond. The molecules show short intramolecular H···I contacts of 2.89 and 2.92 Å. The crystal packing shows no short intermolecular contacts. In KABKAB, there are four molecules per unit cell. The symmetrical molecules are arranged in a herringbone fashion (Koren *et al.*, 2003) in which the molecules are packed in an edge-to-face orientation. In IDOTOM, the molecules are aligned along the *b*-axis. Four kinds of weak C—H···N interactions are recognized, one of which connects the molecules into a one-dimensional array and the remaining three link these arrays.

Table 3
Experimental details.

Crystal data	
Chemical formula	$C_{25}H_{18}N_6{\cdot}H_2O$
M_r	420.47
Crystal system, space group	Triclinic, $P\overline{1}$
Temperature (K)	100
a, b, c (Å)	10.2188 (5), 10.7365 (5), 20.4119 (10)
α, β, γ (°)	84.376 (2), 89.298 (2), 70.167 (2)
V (Å^3)	2095.97 (18)
Z	4
Radiation type	Mo $K\alpha$
μ (mm^{-1})	0.09
Crystal size (mm)	0.32 × 0.19 × 0.16
Data collection	
Diffractometer	Bruker D8 QUEST PHOTON-III CCD
Absorption correction	Multi-scan (*SADABS*; Krause *et al.*, 2015)
T_{min}, T_{max}	0.834, 0.947
No. of measured, independent and observed [$I > 2\sigma(I)$] reflections	55460, 7385, 5414
R_{int}	0.066
(sin $\theta/\lambda)_{max}$ (Å^{-1})	0.595
Refinement	
$R[F^2 > 2\sigma(F^2)]$, $wR(F^2)$, S	0.049, 0.143, 1.02
No. of reflections	7385
No. of parameters	625
No. of restraints	4
H-atom treatment	H atoms treated by a mixture of independent and constrained refinement
$\Delta\rho_{max}$, $\Delta\rho_{min}$ (e Å^{-3})	0.39, −0.32

Computer programs: *APEX3* (Bruker, 2018), *SAINT* (Bruker, 2013), *SHELXT2014/5* (Sheldrick, 2015*a*), *SHELXL2019/3* (Sheldrick, 2015*b*), *ORTEP-3 for Windows* (Farrugia, 2012) and *PLATON* (Spek, 2020).

5. Synthesis and crystallization

A solution of acetophenone (17 mmol) and malononitrile (26 mmol) in ethanol (35 mL) was stirred for 1 h. Then 5 drops of methylpiperazine were added to the reaction mixture. The resulting reaction mixture was stirred for 4 h. After the reaction was complete, it was kept for 5 days until the formation of crystals occurred. The crystals were separated by filtration and recrystallized from an ethanol–water solution (m.p. = 458–459 K, yield 55%).

^{1}H NMR (300 MHz, DMSO-d_6, ppm.): 2.32 (*s*, 3H, CH_3); 6.88 (*s*, 4H, $2NH_2$); 7.19–7.87 (*m*, 10H, $10CH_{arom.}$); 7.96 (*s*, 1H, NH). ^{13}C NMR (75 MHz, DMSO-d_6, ppm): 17.95 (CH_3), 61.61 ($C_{quat.}$), 67.24 ($C_{quat.}$), 69.98 ($C_{quat.}$), 116.21 (CN), 116.88 (CN), 117.76 (=CH), 119.32 (CN), 127.52 ($2CH_{arom.}$), 127.58 ($CH_{arom.}$), 128.62 ($2CH_{arom.}$), 128.90 ($CH_{arom.}$), 129.37 ($2CH_{arom.}$), 129.54 ($2CH_{arom.}$), 138.14 ($C_{arom.}$), 142.25 ($C_{arom.}$), 145.96 ($C_{quat.}$), 155.03 ($C_{quat.}$), 161.99 ($C_{quat.}$), 166.07 ($C_{quat.}$), 166.39 ($C_{quat.}$).

6. Refinement

Crystal data, data collection and structure refinement details are summarized in Table 3. All C-bound H atoms were placed at calculated positions and refined using a riding model, with

C—H = 0.95–0.98 Å, and with U_{iso}(H) = 1.2 or 1.5U_{eq}(C). The N-bound H atoms were located in difference-Fourier maps and refined freely. The O-bound H atoms were located in difference-Fourier maps and were refined with U_{iso}(H) = 1.5U_{eq}(O). The O—H bond lengths of water molecules were forced to be 0.85 ± 0.02 Å with the DFIX command. Both H atoms of the water molecules were forced to have the same displacement parameters with the EADP command.

Acknowledgements

Authors' contributions are as follows. Conceptualization, IGM, ANK and FNN; methodology, IGM and MA; investigation, VNK and FNN; writing (original draft), MA, AB and ANK,; writing (review and editing of the manuscript), İGM and ANK; visualization, MA, FSK and FNN; funding acquisition, VNK, AB and FNN; resources, AB, VNK and MA; supervision, MA and ANK.

Funding information

This paper was supported by Baku State University and the RUDN University Strategic Academic Leadership Program.

References

Abd El-Lateef, H. M., Khalaf, M. M., Gouda, M., Kandeel, M., Amer, A., Abdelhamid, A. A., Drar, A. M. & Gad, M. A. (2023). *ACS Omega*, **8**, 29685–29692.

Atalay, V. E., Atish, I. S., Shahin, K. F., Kashikchi, E. S. & Karahan, M. (2022). *UNEC J. Eng. Appl. Sci.* **2**, 33–40.

Bats, J. W., Urschel, B. & Müller, T. (2008). *Acta Cryst.* E**64**, o2235.

Bruker (2013). *SAINT*. Bruker AXS Inc., Madison, Wisconsin, USA.

Bruker (2018). *APEX3*. Bruker AXS Inc., Madison, Wisconsin, USA.

Donmez, M. & Turkyılmaz, M. (2022). *UNEC J. Eng. Appl. Sci*, **2**, 43–48.

Farrugia, L. J. (2012). *J. Appl. Cryst.* **45**, 849–854.

Groom, C. R., Bruno, I. J., Lightfoot, M. P. & Ward, S. C. (2016). *Acta Cryst.* B**72**, 171–179.

Ibis, C. & Deniz, N. G. (2006). *Acta Cryst.* E**62**, o5373–o5374.

Ibis, C. & Deniz, N. G. (2007*a*). *Acta Cryst.* E**63**, o1091–o1092.

Ibis, C. & Deniz, N. G. (2007*b*). *Acta Cryst.* E**63**, o4394.

Ibis, C. & Deniz, N. G. (2007*c*). *Acta Cryst.* E**63**, o3058.

Koren, A. B., Curtis, M. D., Francis, A. H. & Kampf, J. W. (2003). *J. Am. Chem. Soc.* **125**, 5040–5050.

Krause, L., Herbst-Irmer, R., Sheldrick, G. M. & Stalke, D. (2015). *J. Appl. Cryst.* **48**, 3–10.

Maharramov, A. M., Shikhaliyev, N. G., Zeynalli, N. R., Niyazova, A. A., Garazade, Kh. A. & Shikhaliyeva, I. M. (2021). *UNEC J. Eng. Appl. Sci.* **1**, 5–11.

Naghiyev, F. N., Akkurt, M., Askerov, R. K., Mamedov, I. G., Rzayev, R. M., Chyrka, T. & Maharramov, A. M. (2020). *Acta Cryst.* E**76**, 720–723.

Naghiyev, F. N., Khrustalev, V. N., Novikov, A. P., Akkurt, M., Rzayev, R. M., Akobirshoeva, A. A. & Mamedov, I. G. (2022). *Acta Cryst.* E**78**, 554–558.

Naghiyev, F. N., Tereshina, T. A., Khrustalev, V. N., Akkurt, M., Rzayev, R. M., Akobirshoeva, A. A. & Mamedov, İ. G. (2021). *Acta Cryst.* E**77**, 516–521.

Narayan, G., Rath, N. P. & Das, S. (2010). *Acta Cryst.* E**66**, o2678.

Okuno, T. & Iwahashi, H. (2013). *Acta Cryst.* E**69**, o665.

Sathiyanarayanan, K., George Fernand, A., Dhanasekaran, V. & Rathore, R. S. (2007). *Acta Cryst.* E**63**, o2504–o2505.

Sathiyanarayanan, K., George Fernand, A., Dhanasekaran, V. & Rathore, R. S. (2008*a*). *Acta Cryst.* E**64**, o124.

Sathiyanarayanan, K., George Fernand, A., Dhanasekaran, V. & Rathore, R. S. (2008*b*). *Acta Cryst.* E**64**, o123.

Sheldrick, G. M. (2015*a*). *Acta Cryst.* A**71**, 3–8.

Sheldrick, G. M. (2015*b*). *Acta Cryst.* C**71**, 3–8.

Sobhi, R. M. & Faisal, R. M. (2023). *UNEC J. Eng. Appl. Sci.* **3**, 21–32.

Spackman, P. R., Turner, M. J., McKinnon, J. J., Wolff, S. K., Grimwood, D. J., Jayatilaka, D. & Spackman, M. A. (2021). *J. Appl. Cryst.* **54**, 1006–1011.

Spek, A. L. (2020). *Acta Cryst.* E**76**, 1–11.